J Arid Land (2025) 17(6): 754–771
doi: 10.1007/s40333-025-0016-8; CSTR: 32276.14.JAL.02500168

Science Press Springer-Verlag

Spatial and temporal evolution of forage-livestock balance in the agro-pastoral transition zone of northern China

LIU Huan[1], YAO Yuyan[2], AI Zemin[1*], DANG Xiaohu[3], CAO Yong[1], LI Qingqing[1], HOU Mengjia[1], HU Haoli[1], ZHANG Yuanyuan[1], CAO Tian[1]

[1] College of Geomatics, Xi'an University of Science and Technology, Xi'an 710054, China;
[2] Natural Resources Agency, Sanyuan County, Xianyang 713800, China;
[3] College of Geology and Environment, Xi'an University of Science and Technology, Xi'an 710054, China

Abstract: Research on grassland carrying capacity (GCC) and forage-livestock balance is of great significance for promoting the harmonious development of human and grassland. However, the lack of understanding of GCC and forage-livestock balance in the agro-pastoral transition zone of northern China has limited the grassland sustainable development. Here, the spatial and temporal characteristics of GCC and forage-livestock balance in the grassland of agro-pastoral transition zone of northern China from 2000 to 2022 were analyzed using meteorological data and remote sensing data. Geographical detectors and geographically weighted regression were also used to identify the driving factors and their interactions with GCC changes. Moreover, future GCC trends were predicted using the Coupled Model Intercomparison Project Phase 6 dataset. Results revealed that: (1) GCC showed an overall upward trend from 2000 to 2022 but with significant inter-annual fluctuations. Its spatial distribution decreased gradually from north to south and from east to west. Precipitation, temperature, and cumulative solar radiation were the main drivers of the inter-annual variation of GCC, and the interaction between precipitation and temperature was the main influencing factor of the spatial distribution of GCC; (2) the forage-livestock balance was in an overloaded state in most years, but its index remained basically stable. Spatially, grazing overloading was mainly distributed in northeastern area and the severe overloading was mainly distributed in northwestern area; and (3) future projections indicated a downward trend in potential GCC. Under shared socioeconomic pathway (SSP)2-4.5 scenario, the potential GCC had a ranged of 1.38×10^7–1.86×10^7 standard sheep unit (SHU) and a mean of 1.60×10^7 SHU. Meanwhile, the potential GCC under SSP5-8.5 scenario had a range of 1.18×10^7–1.69×10^7 SHU and a mean of 1.49×10^7 SHU. These results indicated that although GCC of the agro-pastoral transition zone of northern China showed an overall increasing trend from 2000 to 2022, the forage-livestock balance index remained basically stable. The GCC was predicted to show a decreasing trend in the future. The findings provide a scientific basis for the sustainable development of grassland and the optimization of grazing management policies in this area.

Keywords: grassland carrying capacity; climate change; forage-livestock balance; grassland ecosystem; grazing management

Citation: LIU Huan, YAO Yuyan, AI Zemin, DANG Xiaohu, CAO Yong, LI Qingqing, HOU Mengjia, HU Haoli, ZHANG Yuanyuan, CAO Tian. 2025. Spatial and temporal evolution of forage-livestock balance in the agro-pastoral transition zone of northern China. Journal of Arid Land, 17(6): 754–771. https://doi.org/10.1007/s40333-025-0016-8; https://cstr.cn/32276.14.JAL.02500168

*Corresponding author: AI Zemin (E-mail: aizmxs@yeah.net)
Received 2024-11-06; revised 2025-03-27; accepted 2025-04-09

1 Introduction

Grasslands are one of the most important terrestrial ecosystems on Earth because they regulate global climate change, prevent the advancement of desertification, maintain biodiversity, and serve as the material basis for the survival of pastoralists (Petermann and Buzhdygan, 2021; He et al., 2023). Therefore, the sustainable development of grassland ecosystems is crucial for ensuring global ecosystem balance and promoting the sustainable development of livestock husbandry (Erb et al., 2018). However, the functional diversity and integrity of grassland ecosystems have been severely influenced by human activities (such as grazing, tillage, and mowing) and climate change (Zeng et al., 2014; Jordon et al., 2024), resulting in varying degrees of degradation. Among the factors contributing to grassland degradation, overgrazing is an important factor in the decline of vegetation cover, destruction of topsoil structure, and compaction of soil (Romero-Ruiz et al., 2023; Guo and Chen, 2024). Overgrazing usually occurs when the actual carrying capacity exceeds the grassland carrying capacity (GCC) and seriously restricts the sustainable utilization of grassland resources (Huang et al., 2021). Therefore, the coordinated development of grassland ecosystems and livestock husbandry has become an important issue in the research of grassland sustainable development (Du et al., 2022; Li et al., 2022).

GCC refers to the ability of grassland resources in the area to carry the largest population, livestock, and economic production for sustainable utilization (Guevara et al., 1997; Yan et al., 2023). As an indicator to quantify grassland productivity, it is of paramount importance in ecologically sustainable stocking rates that take into account vegetation production, regional ecology, and livestock needs (Qian et al., 2012). Grassland degradation, land desertification, biodiversity loss, and other problems occur when the actual carrying capacity exceeds GCC (Wei et al., 2022). Therefore, the timely and accurate understanding of GCC is essential for the formulation of rational grassland grazing management policies. The net primary productivity (NPP) of vegetation takes into account plant growth, respiration, and nutrient utilization. It is a direct factor of grassland productivity and can be used to assess the potential food supply of livestock, thus helping to determine GCC (De Leeuw et al., 2019; Yan et al., 2023). Researchers estimate mainly GCC at large regional scales based on remote sensing data (Ba et al., 2023; Wang et al., 2024b). For example, the Carnegie Ames Stanford Approach (CASA) model was used by Du et al. (2024) to estimate GCC, and it was found that theoretical carrying capacity of the grasslands in the Qilian Mountains, China showed a significant increasing trend from 2000 to 2018. Another study evaluated the GCC of Azerbaijani grasslands on the basis of grass production and found that a reasonable GCC allowed only 65.00% of aboveground biomass to be consumed (De Leeuw et al., 2019). Li et al. (2024) examined the GCC in Eastern Mongolian Plateau based on remote sensing data and clarified the influence factors of GCC. The main factors driving GCC changes are receiving increasing attention from researchers. For example, studies of GCC in Tajikistan and Kyrgyzstan have shown that human overgrazing and climate change are the main factors influencing changes in GCC (Umuhoza et al., 2021). A study of the Xizang Plateau in China found synergistic effects of climate change and ecological conservation on GCC (Yan et al., 2024). Studies have confirmed the role of human activities and climate change in influencing GCC. To quantitatively evaluate the balance between GCC and actual carrying capacity, scholars introduced the forage-livestock balance concept (Dong et al., 2002; Mai et al., 2013). The core of this concept is to evaluate the relationship between grass and livestock based on the amount of grass, GCC, and actual livestock load (Wang and Liu, 2017). Based on remote sensing data and ground surveys on forage livestock balance, Xiong et al. (2025) found that Wensu County in northern China had experienced serious overloading in the past 23 a, and Qu et al. (2021) found that the grassland area of Xilingol League in China had been overloaded from 2000 to 2015, accounting for 50.00% of the study area. The clear equilibrium distribution and overloading of grass and livestock provide an important theoretical basis for the sustainable development of regional animal husbandry. The researchers also modeled and predicted the future trend of GCC (Zhang et al., 2023; Shi et al., 2024; Wang et al., 2024a), and the results of the simulation can

provide important theoretical support for the optimization of regional grazing management policies.

As a typical ecologically fragile zone, the agro-pastoral transition zone of northern China is an important livestock production base and ecological barrier area in the country (Yang et al., 2020; Guo et al., 2023; Dai et al., 2024; Yang et al., 2024). As a traditional and important economic activity, grazing exerts a determinant influence on the structure and function of regional ecosystems through its intensity and management practices. For the agro-pastoral transition zone of northern China, researchers studied the effects of grazing on *Stipa baicalensis* Roshev. grasslands (Jin and Han, 2010), Hulunbuir grasslands (Zhu et al., 2022), and grasslands in Inner Mongolia (Su et al., 2017) and found that grazing overloads the grasslands to varying degrees. However, most of these studies focused on grazing in a small area scale and lacked a comprehensive examination of the entire area. Furthermore, their results lacked a predictive analysis of potential future GCC changes, which reduces the potential as a reference for prospective government decisions. Therefore, research on GCC, forage-livestock balance, and determinant factors in the agro-pastoral transition zone of northern China is essential to promote the ecological protection and restoration of this area and its sustainable social and economic development. Studies on small areas showed that GCC increased (Song et al., 2018; Li et al., 2024) and most of these areas were overloaded (Su et al., 2017; Zhu et al., 2022). Hence, we hypothesized that GCC in the agro-pastoral transition zone of northern China followed a general upward trend from 2000 to 2022, and the forage-livestock balance was overloaded. Meanwhile, we explored the main factors influencing GCC and forecasted the future trend of GCC in the area.

2 Materials and methods

2.1 Study area

The study area is located between 35°30′–45°30′N and 105°55′–124°00′E, with a total area of 813.4×10^3 km^2, which includes the Inner Mongolia Autonomous Region, Shaanxi Province, Liaoning Province, Shanxi Province, Gansu Province, Ningxia Hui Autonomous Region, and Hebei Province (Fenetahun et al., 2022). The agro-pastoral transition zone of northern China is located in the temperate continental monsoon climate zone, with high temperature and rain in summer and cold and dry in winter (Yang et al., 2024). Precipitation is concentrated in July and August, decreasing from southeast to northwest. Fluctuations between dry and wet conditions are evident, reflecting the unique characteristics of the East Asian monsoon climate (Bai et al., 2022). The annual average temperature ranges from 2°C to 8°C and the average annual precipitation ranges from 300 to 500 mm.

2.2 Data source

2.2.1 Remote sensing data

Surface solar radiation data were obtained from the National Tibetan Plateau Science Data Center (Table 1). Temperature data with a spatial resolution of 1 km were acquired from the China Regional Monthly Mean Temperature Dataset from 1901 to 2022. Precipitation data with a spatial resolution of 1 km were derived from the China Regional Monthly Precipitation Dataset from 1901 to 2022. Potential evapotranspiration (PET) data were sourced from PET dataset for China from 1990 to 2022, which was calculated using the Hargreaves formula and by the monthly minimum, average, and maximum air temperature data. Normalized difference vegetation index (NDVI) data with a spatial resolution of 250 m were obtained from the monthly NDVI products for China from 2000 to 2022. Land use data with a spatial resolution of 30 m were obtained from the annual China land cover dataset. The dataset contains 9 land cover classifications, namely, cropland, woodland, shrubland, grassland, water body, permanent snow and glaciers, vacant land, impervious surface, and wetland. The NPP data with a spatial resolution of 500 m were obtained from the Moderate Resolution Imaging Spectroradiometer (MODIS) Tera NPP gap-filled yearly L4 global 500 m Sinusoidal grid product, derived from the Terra sensor on the National

Aeronautics and Space Administration (NASA) platform. Slope length data were derived from elevation data using the data analysis tool of ArcGIS v.10.4 software (Environmental Systems Research Institute Inc. (ESRI), Redlands, USA). Remote sensing data with various resolutions were resampled to a uniform resolution of 500 m for analysis using ArcGIS.

Annual livestock inventory data from the cities and counties in the agro-pastoral transition zone of northern China from 2000 to 2022 were collected to quantitatively assess the spatiotemporal characteristics of forage-livestock balance. In this study, the livestock inventory was converted into standard sheep unit (SHU), following the method outlined in the Agricultural Industry Standard of China. During the conversion, the conversion factor was set as 4.0 for large livestock and 1.0 for sheep (Su et al., 2002).

Table 1 Remote sensing data source

Data name	Time sale	Resolution	Data source
Accumulated solar radiation	2000–2022	3 h, 10 km	https://data.tpdc.ac.cn
Precipitation	1901–2022	1 km	https://data.tpdc.ac.cn
Temperature	1901–2022	1 km	https://data.tpdc.ac.cn
Potential evapotranspiration (PET)	1990–2022	1 km	https://data.tpdc.ac.cn
Relative humidity	2000–2022	1 km	https://data.tpdc.ac.cn
Normalized difference vegetation index	2000–2022	250 m	https://data.tpdc.ac.cn
Land use data	2000–2022	30 m	https://www.ngcc.cn/zdchgc/qqdbfg
Digital elevation model (DEM)	2000–2022	30 m	https://www.gscloud.cn
Slope	2000–2022	30 m	https://www.gscloud.cn
Slope length	2000–2022	30 m	https://www.gscloud.cn
Vegetation type	2000–2022	1:1,000,000	https://www.resdc.cn
Gross domestic product (GDP)	2000–2022	1 km	http://gis5g.com
Population distribution	2000–2022	1 km	http://gis5g.com
Nighttime Light	2000–2022	1 km	http://gis5g.com
Net primary productivity (NPP)	2000–2022	500 m	https://www.nasa.gov
Soil texture	2006	1 km	https://data.tpdc.ac.cn/home
Grassland type	-	1 km	http://www.gisrs.cn

Note: "-" indicates no time scale.

2.2.2 Data for future scenario

The corrected NASA Earth Exchange Global Daily Scale Prediction dataset from the Coupled Model Intercomparison Project Phase 6 (CMIP6) was used as future scenario. Future temperature and precipitation data from the shared socioeconomic pathway (SSP)2-4.5 and SSP5-8.5 scenarios were used to estimate the NPP in the study area. The potential GCC was then predicted using the estimated NPP data (Table 2).

Table 2 Coupled Model Intercomparison Project Phase 6 (CMIP6) model data parameters from 2024 to 2030

Data name	Description	Resolution	Data source
Historical data	The time scale is from 2000 to 2014.	25 km	https://registry.opendata.aws/nex-gddp-cmip6
SSP2-4.5	Future scenario data, moderate radiative forcing scenario with radiative forcing reaching 4.5 W/m^2 by 2100		
SSP5-8.5	Future scenario data, high level radiative forcing scenario with radiative forcing reaching 8.5 W/m^2 by 2100		

Note: SSP, shared socioeconomic pathway.

2.3 Methods

2.3.1 Grassland yield

Grassland yield, defined as the total amount of dry matter produced in a given area over a specific period, is a key indicator for assessing the production capacity of grassland ecosystems (Jin et al., 2011). In this study, we extracted land use data for grasslands based on the land classes of grasslands in the study area. NPP was then estimated using the Carnegie-Ames-Stanford Approach (CASA) model. The estimated NPP values were superimposed on grassland yield data to obtain the actual NPP from 2000 to 2022. Actual NPP was further used to calculate the grassland yield per unit area, using the following formula (Zhu et al., 2022):

$$B_g = \frac{\text{NPP}}{S_{\text{bn}}\left(1+S_{ug}\right)}, \tag{1}$$

where B_g is the total annual hay production per unit area (g/(m^2·a)); NPP is the total annual net primary production of grasslands (g C/(m^2·a)); S_{bn} is the conversion coefficient of grassland biomass converted into NPP (0.45 g/g C) (Zhu et al., 2022); and S_{ug} is the ratio coefficient of belowground to aboveground biomass for different grassland types (Chen et al., 2008; Zhang et al., 2016), which is shown in Table 3.

Table 3 Ratio coefficients of belowground to aboveground biomass for different grassland types

Grassland type	Ratio coefficient of belowground to aboveground biomass	Grassland type	Ratio coefficient of belowground to aboveground biomass
Temperate desert	7.89	Temperate desert steppe	7.89
Temperate steppe desert	7.89	Temperate grassland	4.42
Scrub	4.42	Temperate meadow	6.31
Temperate meadow grassland	5.26	Alpine meadow	8.99
Temperate typical grassland	4.25	Swamp	15.68

2.3.2 GCC

GCC was calculated by combining the yield of edible pasture with the daily consumption of livestock (Chen, 2005, 2008). The formula can be expressed as follows:

$$\text{GCC} = \frac{H_{\text{g}} \times K_1 \times K_2 \times K_3}{L_{\text{g}} \times d}, \tag{2}$$

where GCC is the grassland carrying capacity (SHU); H_g is the annual grassland hay yield (g/m^2); K_1 is the utilization rate of different grassland types: 50.00% for grassland, 60.00% for meadow, 55.00% for irrigated grass bushes and swamps, and 40.00% for desert; K_2 is the utilization rate of grassland with a value of 85.00%; K_3 is the edible grass coefficient of grassland with a value of 80.00%; L_{g} is the daily feed intake of a sheep unit with a value of 2 kg/(SHU·d); and d is the grazing period, calculated for 365 d of the year.

2.3.3 Forage-livestock balance index

Grazing overload rate was used to measure the forage-livestock balance in the study area and was calculated as follows (Xu and Yang, 2009; Xu et al., 2012):

$$C = \frac{C_S - C_h}{C_h} \times 100\%, \tag{3}$$

where C is the grazing overload rate (%); C_S is the actual livestock load (SHU/hm^2); and C_h is the GCC per unit area (SHU/hm^2). The forage-livestock balance was categorized into five levels: insufficient GCC ($C \leq -10.00\%$), forage-livestock balance ($-10.00\% < C \leq 10.00\%$), critical overload ($10.00\% < C \leq 20.00\%$), overload ($20.00\% < C \leq 50.00\%$), and severe overload ($C > 50.00\%$) (Liu et al., 2018).

2.3.4 Supplementary feeding

The supplementary feeding of agricultural by-products comprises two parts: concentrate fodder and roughage. Concentrate fodder mainly includes bran and rape oil cake, and roughage mainly includes straw. The daily feed intake for each standard goat is 1.0 kg of concentrate fodder or 1.5 kg of roughage (Yang and Yang, 2000; Li et al., 2012). In this study, we calculated the amount of supplementary feeding based on annual supplementation (365 d).

2.3.5 Simulation and prediction of grassland NPP

The model of Zhou et al. (1998) was adopted to estimate grassland NPP, using the vegetation CO_2 flux and water vapor flux equation. The model of Zhang et al. (2011) was used to calculate vegetation productivity and to verify the simulation results for Zalong Wetland, China (Yu et al., 2021). The calculation formulas are as follows:

$$\mathrm{NPP} = \mathrm{RDI}^2 \frac{r\left(1+\mathrm{RDI}+\mathrm{RDI}^2\right)}{\left(1+\mathrm{RDI}\right)\left(1+\mathrm{RDI}^2\right)\exp\left[-\left(\mathrm{a}+\mathrm{bRDI}\right)^{0.5}\right]}, \tag{4}$$

$$\mathrm{RDI} = \left(\mathrm{c}+\mathrm{dPER}-\mathrm{ePER}^2\right)^2, \tag{5}$$

$$\mathrm{PER} = \frac{\mathrm{PET}}{r} = \frac{\mathrm{fBT}}{r}, \tag{6}$$

$$\mathrm{PET} = 58.931\mathrm{BT}, \tag{7}$$

$$\mathrm{BT} = \frac{\sum t}{365} = \frac{\sum T}{12}, \tag{8}$$

where RDI is the radiation dryness index; r is the annual precipitation (mm); a, b, c, d, e, and f are the constants, which are 9.87, 6.25, 0.629, 0.237, 0.00313, and 58.931, respectively; PER is the possible evaporation rate; PET is the potential evapotranspiration (mm); BT is the average annual biological temperature (°C); t is the average daily temperature of less than 30°C and greater than 0°C; and T is the average monthly temperature of less than 30°C and greater than 0°C.

2.3.6 Statistical analysis

Pearson correlation analysis was used to quantify the effects of precipitation and temperature on vegetation NPP. The correlation coefficient R^2 ranges from –1 to 1, where a larger absolute value of R^2 indicates a strong correlation between vegetation NPP and the influencing factors of precipitation or temperature (Sedgwick, 2012; Ma et al., 2023).

The geographical detector is a statistical tool proposed by Wang and Xu (2017) to explore the spatial stratified heterogeneity of geographical elements and identify their influencing factors. It quantifies the effect of multiple independent variables on a dependent variable using a significance test. The q-value that is the influence of independent variables on dependent variables can be calculated as follows (Dai and Wang, 2020):

$$q = 1 - \frac{\sum_{k=1}^{L} N_k \sigma_k^2}{N\sigma^2}, \tag{9}$$

where L is the classification or stratification of the independent variable; k is the stratification of livestock load or different driving factors; N_k is the number of hierarchical image elements of each data stratum; σ_k^2 is the variance of each level of image element of each data stratum; N is the number of all image elements; and σ^2 is the variance of all image metadata in the study area. The q-value, which ranges from 0 to 1, indicates the degree of spatial stratified heterogeneity and the contribution of driving factors to the livestock load. A large q-value suggests a great contribution of the driving factor to the livestock load and a significant spatial difference, and a small q-value indicates a weak contribution.

Geographically weighted regression (GWR) is used to model the relationship between a dependent variable and independent variables within a localized area. GWR provides insights into spatial heterogeneity, characterizing how a variable, such as GCC, is influenced by the explanatory variables, such as cumulative solar radiation, precipitation, and relative humidity. The model can be expressed as follows (Brunsdon et al., 1996):

$$Y_i = \beta_0(u_i, v_i) + \sum_{i=1}^{k} \beta_k(u_i, v_i) x_{ik} + \varepsilon_i, \tag{10}$$

where Y_i is the satellite precipitation of position i; u_i and v_i are the horizontal and vertical coordinate of position i, respectively; $\beta_0(\mu_i,v_i)$ is the constant term of the model at the i^{th} sample point; k is the number of independent variables; i is the number of samples; $\beta_k(\mu_i,v_i)$ is the regression coefficient for the k^{th} independent variable at point i; x_{ik} is the k^{th} independent variable at the i^{th} sample point; and ε_i is the random error term for sample point i. Given that GCC is characterized by spatial autocorrelation and spatial non-stationarity, we utilized a GWR model to explain the geospatial relationship between GCC and natural factors (cumulative solar radiation, precipitation, and relative humidity).

First, the ordinary least squares (OLS) method was used to conduct significance test and linearity check among these variables. The mean value of GCC, cumulative solar radiation, precipitation, and relative humidity from 2000 to 2022 in the agro-pastoral transition zone of northern China were used as gridded data to generate 11,140 grid points. At each grid point, corresponding values of GCC, cumulative solar radiation, precipitation, and relative humidity were available. GWR models were then employed to investigate the local spatial correlations between the changes in GCC and each meteorological factor (cumulative solar radiation, precipitation, and relative humidity) to reveal the spatial heterogeneity of interactions among these variables.

3 Results

3.1 Spatiotemporal variation of GCC

GCC in the agro-pastoral transition zone of northern China exhibited an overall upward trend (Fig. 1). It was the largest in 2022, which increased by 66.31% compared with that in 2000. GCC also exhibited a fluctuating growth trend in the past 23 a, with marked declines in 2007, 2009, 2015, 2017, and 2020, and notable increases in 2004, 2008, 2013, 2017, 2019, and 2022.

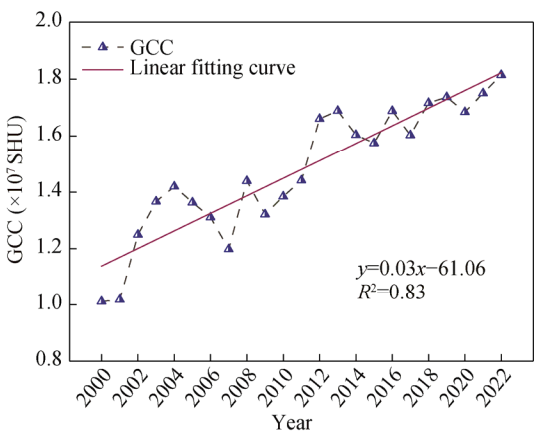

Fig. 1 Annual variation of grassland carrying capacity (GCC) in the agro-pastoral transition zone of northern China. SHU, standard sheep unit.

Spatial distribution of average GCC in the agro-pastoral transition zone of northern China greatly varied from 2000 to 2020, showing a distribution pattern with "northeast-southwest" as the

axis. GCC values were higher in the south and east, and lower in the west and north (Fig. 2). Areas with high GCC were found in Shaanxi and Hebei provinces. Areas with medium GCC were located in the southern Ningxia Hui Autonomous Region, Gansu Province, central Shaanxi Province, Shanxi Province, Hebei Province, Liaoning Province, and most parts of the Inner Mongolia Autonomous Region. Areas with low GCC were distributed in the northern Ningxia Hui Autonomous Region, northwestern Shanxi Province, and northwestern Inner Mongolia Autonomous Region.

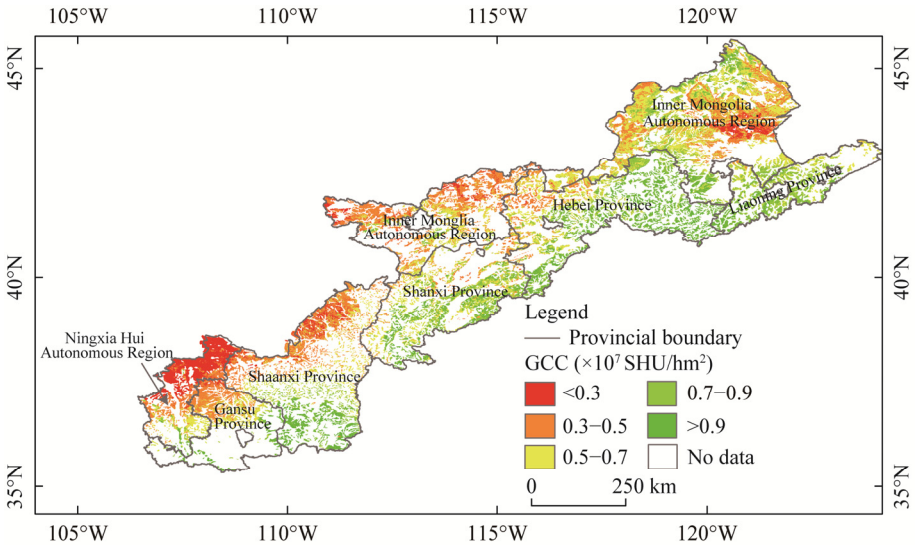

Fig. 2 Spatial distribution of GCC in the agro-pastoral transition zone of northern China from 2000 to 2022. Note that the map is derived from the Geographical Information Monitoring Platform (http://www.dsac.cn) and the boundaries of provinces and autonomous regions are not revised.

3.2 Driving factors of GCC

The selected natural and socio-economic factors, except for nighttime light, passed the significance test (P<0.05), indicating their effects on GCC changes. The q-value of each factor for the spatial distribution of GCC from 2000 to 2022 was sorted as: accumulated solar radiation> relative humidity>precipitation>slope>population distribution>PET>terrain undulation>digital elevation model (DEM)>gross domestic product (GDP)>temperature>nighttime light (Fig. 3). Among them, accumulated solar radiation and precipitation had strong interactions with the other factors. In particular, the interactive driving interpretation of cumulative solar radiation∩relative humidity (q=0.62) and accumulated solar radiation∩precipitation (q=0.56) was the strongest. From 2000 to 2022, the accumulated solar radiation and precipitation had the greatest effect on GCC in the agro-pastoral transition zone of northern China (Fig. 4). In particular, accumulated solar radiation mainly had a positive effect on GCC, with regression coefficients ranging from –0.19 to 0.17. Precipitation was strongly positively correlated with GCC, with regression coefficients ranging from –0.03 to 0.02. Positive effects were observed in areas with abundant precipitation and relatively high altitude, and negative effects were limited to a small area in Shaanxi Province. By contrast, the impact of relative humidity on GCC was weaker than those of accumulated solar radiation and precipitation. Its effects were positive and negative, with regression coefficients ranging from –0.03 to 0.28. However, the negative effects were slightly pronounced and exhibited significant spatial variability. For most factor interactions, the q-values of multi-factors combinations were higher than those of single factors, indicating their stronger correlation with GCC.

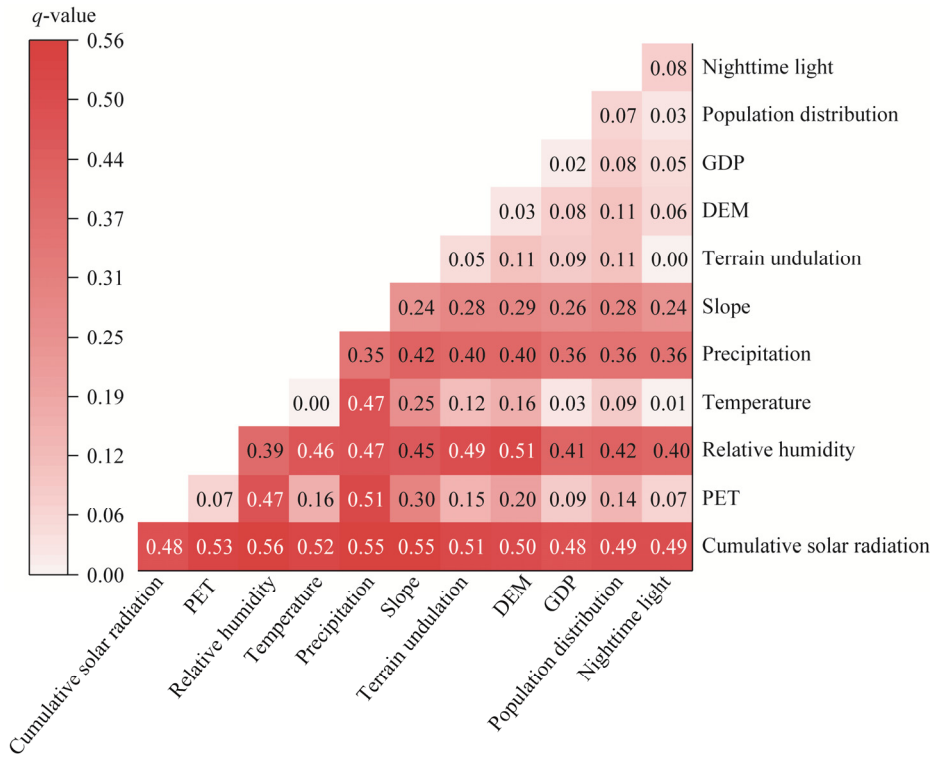

Fig. 3 Geographical detector of driving factors in GCC from 2000 to 2022. DEM, digital elevation model; GDP, gross domestic product. PET, potential evapotranspiration.

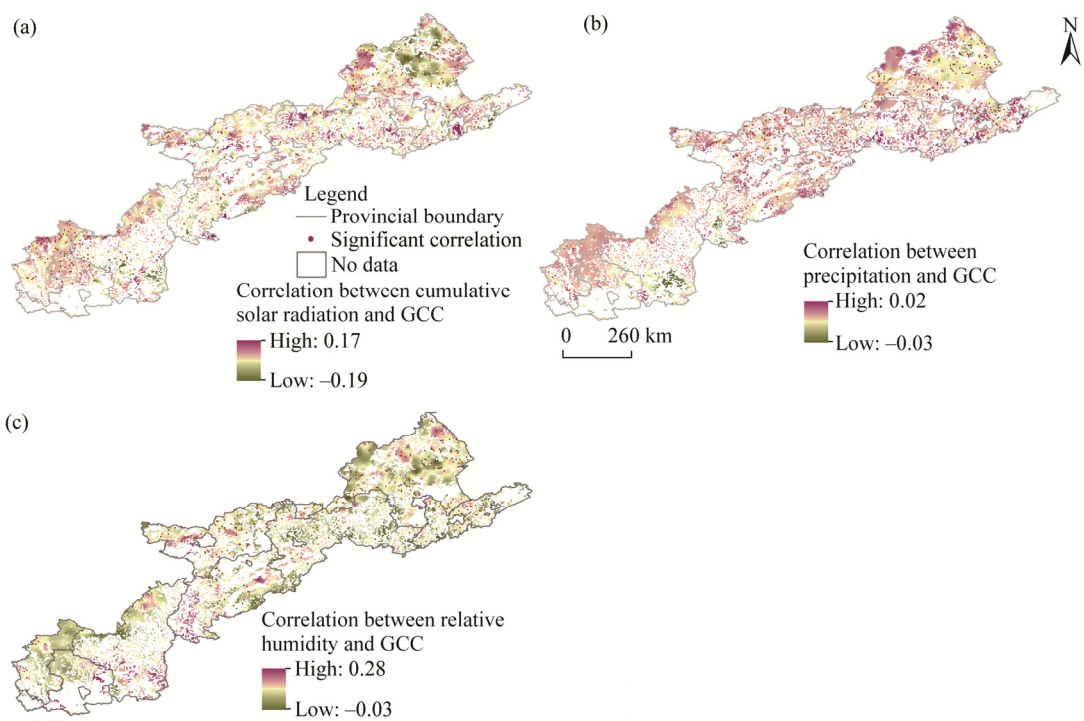

Fig. 4 Spatial heterogeneity of driving factors in GCC in the agro-pastoral transition zone of northern China from 2000 to 2022. (a), cumulative solar radiation; (b), precipitation; (c), relative humidity.

3.3 Spatial and temporal distribution of forage-livestock balance

The forage-livestock balance index in the agro-pastoral transition zone of northern China exhibited a fluctuating upward trend from 2000 to 2022, and the grazing status was predominantly characterized by overloaded and severely overloaded conditions (Fig. 5). The years 2000, 2001, 2006, 2009, and 2015 were classified as severely overloaded, with the highest overload rate reaching 64.43% in 2009. In 2019, the value reached a critical overload level of 18.47%, and all other years experienced varying degrees of overload.

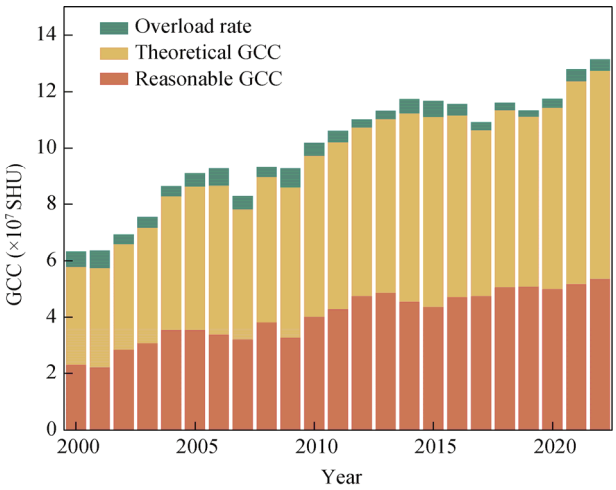

Fig. 5 Distribution of forage-livestock balance index in the agro-pastoral transition zone of northern China from 2000 to 2020. Reasonable GCC indicates the total of theoretical GCC and supplementary feeding amount.

Spatially, the insufficient GCC displayed a stepwise distribution pattern from southwest to northeast, primarily concentrated in Gansu Province, Shaanxi Province and other areas (Fig. 6). Severely overloaded areas were mainly distributed in the northwest, encompassing Ningxia Hui Autonomous Region, Gansu Province, northern Shaanxi Province, parts of Shanxi Province, and Inner Mongolia Autonomous Region. Overloaded areas were scattered across the study area, extending from southwest to northeast. Critical overload areas were relatively limited and primarily located in Hebei Province, central Shaanxi Province, Inner Mongolia Autonomous Region, Liaoning Province, and parts of Gansu Province. Only a few areas, mainly in Shanxi Province, maintained forage-livestock balance.

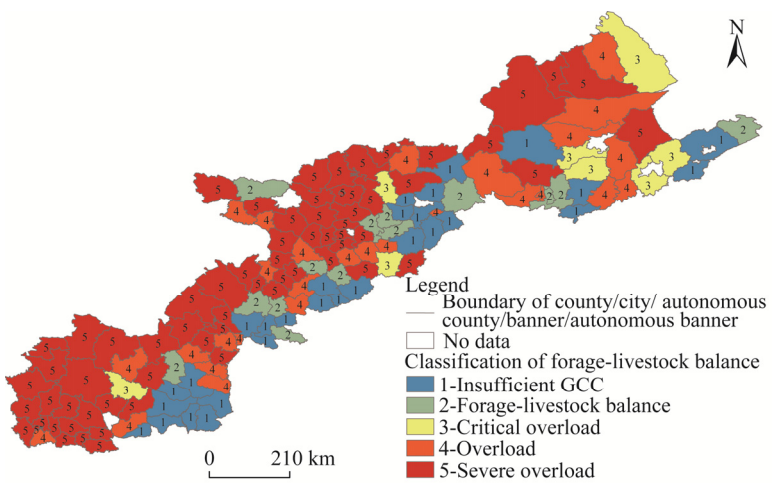

Fig. 6 Distribution of forage-livestock balance map of the agro-pastoral transition zone of northern China from 2000 to 2022.

3.4 Future forecast of potential GCC

Potential GCC in the agro-pastoral transition zone of northern China (R^2=0.72, P<0.05) was calculated using CMIP6 future scenario data and natural vegetation primary productivity model (Fig. 7a). The annual average value of historical potential GCC under CMIP6 climate scenario was 1.46×10^7 SHU, showing no significant difference from the existing GCC (1.37×10^7 SHU). This finding indicated that CMIP6 model had high applicability for predicting potential GCC in the agro-pastoral transition zone of northern China under future climate scenarios. Under SSP2-4.5 scenario, potential GCC had a range of 1.38×10^7–1.86×10^7 SHU and an annual average of 1.60×10^7 SHU. Under SSP5-8.5 scenario, potential GCC had a range of 1.18×10^7–1.69×10^7 SHU, and an average of 1.49×10^7 SHU. Potential GCC under both scenarios was expected to exhibit a fluctuating downward trend in the future. However, potential GCC under SSP2-4.5 scenario would be higher than that under SSP5-8.5 scenario in 2028 (Fig. 7b).

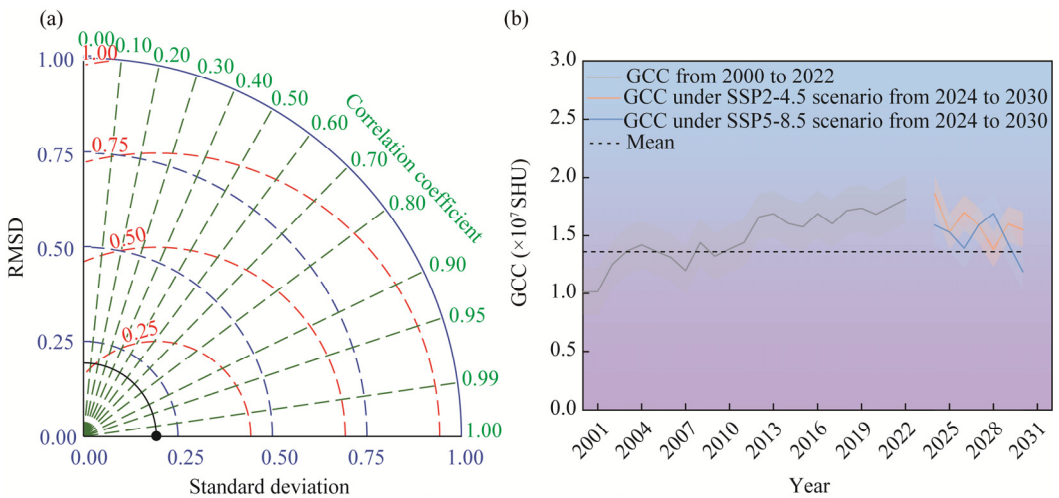

Fig. 7 Taylor diagram of Coupled Model Intercomparison Project Phase 6 (CMIP6) climate model (a) and time variation of GCC in the agro-pastoral transition zone of northern China from 2000 to 2030 (b). The red dashed line in Figure 7a indicates the root mean square error, the black solid line indicates the numerical curve of the simulated standard deviation of the model, and the black dot is the corresponding value of the curve. The same color coverage area in Figure 7b means the standard error of the mean. RMSD, root mean square deviation.

The areas with high potential GCC were expected to be concentrated in Liaoning Province, eastern Hebei Province, and Shaanxi Province in the agro-pastoral transition zone of northern China, and areas with low potential GCC located primarily in the north (Fig. 8). Under SSP2-4.5 scenario, a remarkable change in the spatial distribution of potential GCC would occur in 2028. In this year, areas with high potential GCC would be mainly distributed in Shanxi Province, Hebei Province, and Inner Mongolia Autonomous Region. Areas with high potential GCC would exhibit a northward movement trend. However, this trend might gradually revert to previous trend in 2029 (Fig. 8a–g). Under SSP5-8.5 scenario, spatial distribution of potential GCC in the agro-pastoral transition zone of northern China was projected to follow a "northeast-southwest" axis, with high potential GCC in east and south and low potential GCC in the west and north (Fig. 8h–n).

4 Discussion

4.1 Spatiotemporal variation of GCC

GCC in the agro-pastoral transition zone of northern China generally showed an upward trend over the study period, which was consistent with our hypothesis. In arid and semi-arid areas, precipitation is the main limiting factor for the vegetation growth of grasslands (Zhang et al.,

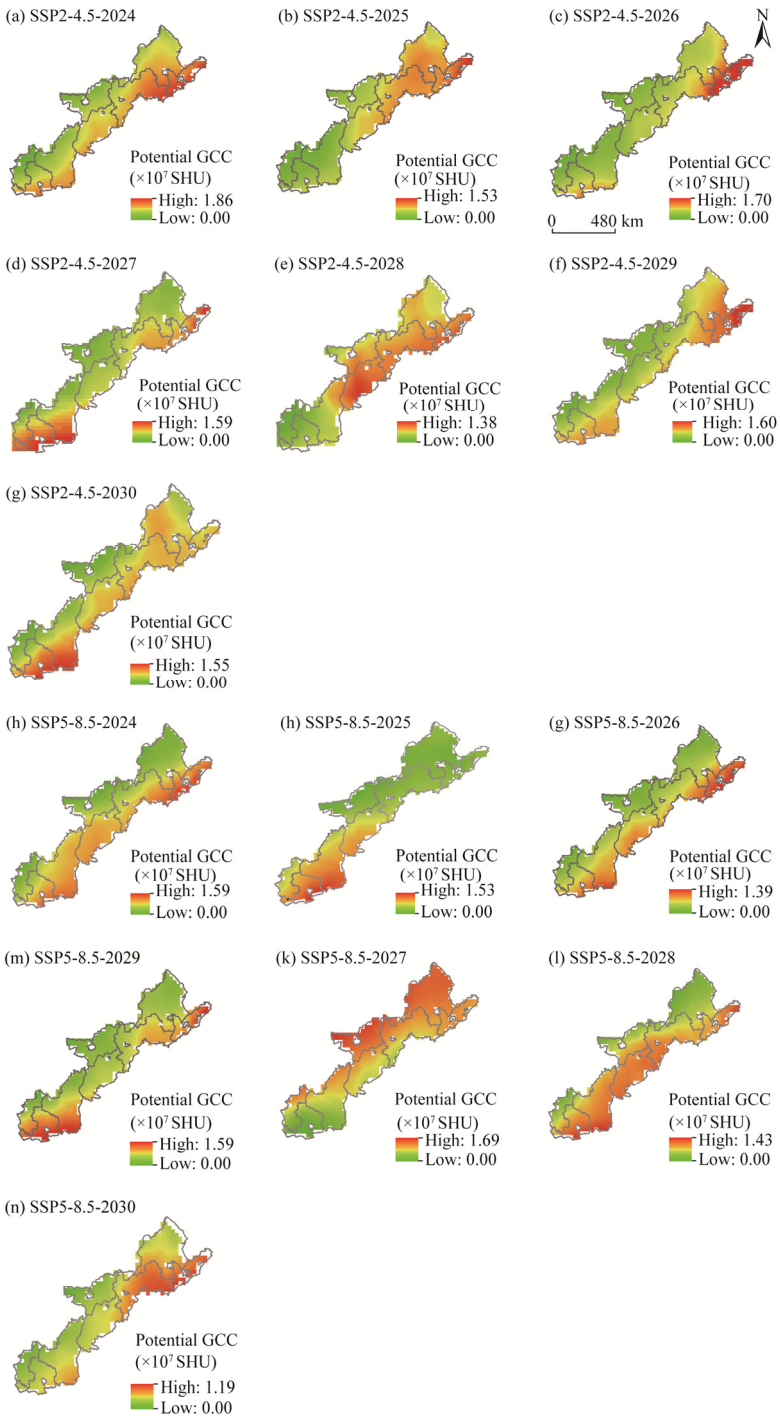

Fig. 8 Spatial distribution of potential GCC under shared socioeconomic pathway (SSP)2-4.5 (a–g) and SSP5-8.5 (h–n) scenarios from 2024 (SSP2-4.5-2024 or SSP5-8.5-2024) to 2030 (SSP2-4.5-2030 or SSP5-8.5-2030)

2022), and the effect of precipitation on vegetation is ultimately reflected in GCC (Chen et al., 2018; Huang et al., 2019; Wen et al., 2019; Chen et al., 2020). Our study also confirmed that the increase in precipitation led to an increase in GCC (r=0.641, P<0.001). However, the uneven inter-annual distribution of precipitation resulted in a decrease in GCC in some years. Researchers found a strong lag effect of drought on grasslands, where the lag effect caused by drought in

previous year reduced grass productivity and led to a decrease in GCC in the following year (Fuchslueger et al., 2016; Hahn et al., 2021; Li et al., 2023). Thus, droughts in 2006, 2008, and 2019 resulted in low GCC in 2007, 2009, and 2020, respectively. However, the lag effect of drought in 2012 and 2016 did not cause the decline in GCC in 2013 and 2017. The main reason may be that the grassland ecological subsidy and incentive policies, such as the forage-livestock balance and audit approval requisition and occupation of grassland, which were introduced and implemented by Chinese government in 2011 and 2015, have contributed to the restoration of grassland ecosystems (Liu et al., 2021). Hence, GCC had been improved to a certain extent.

Areas with high GCC in the agro-pastoral transition zone of northern China were mainly distributed in eastern and southern areas, such as central Shaanxi Province and eastern and northern areas of Hebei Province. Conversely, areas with low GCC were mainly located in western and northern area, including northern Ningxia Hui Autonomous Region, northwestern Shanxi Province, and northwestern Inner Mongolia Autonomous Region. Altitude in eastern and southern areas is low, and high temperatures in these areas can promote the regeneration of grassland vegetation by reducing cold stress and extending the growing season (Xu et al., 2020; Qi et al., 2024). High temperatures also increase photosynthetic efficiency, which in turn favors the growth of grassland vegetation and consequently increases GCC (Dusenge et al., 2019). However, GCC is relatively small in low altitude area of northeastern Inner Mongolia, which is located in the northern agro-pastoral transition zone of northern China. This result can be attributed to the low precipitation in the area, while higher temperatures lead to strong evaporation on the surface, which further reduces soil water content and is not conducive to vegetation growth, resulting in lower GCC (Erb et al., 2018; Jiang et al., 2020). In the high altitude of northern Hebei Province, the intense solar radiation promotes higher grass productivity, which contributes to the increase of GCC in the area (Wen et al., 2019). However, this positive correlation is not absolute, and is significantly regulated by precipitation (Umuhoza et al., 2021). Although solar radiation in northern and western areas of the agro-pastoral transition zone of northern China was relatively high, GCC in this area did not increase with the radiation due to low annual precipitation and intensified vegetation water stress. This finding further confirmed the important role of precipitation and temperature on arid and semi-arid grasslands.

4.2 Temporal and spatial distribution of forage-livestock balance

The agro-pastoral transition zone of northern China has been overloaded in most areas from 2000 to 2022, supporting our hypothesis. Although GCC showed an overall increasing trend, economic development has prompted herders to increase the number of livestock. As a result, the forage-livestock balance index remained in a relatively stable state. A small improvement in the forage-livestock balance in the agro-pastoral transition zone of northern China was observed after 2016. This phenomenon may be attributed to the ecological conservation measures adopted by the government in 2015 (Liu et al., 2021). Achieving regional forage-livestock balance means maintaining a moderate number of livestock, rather than simply reducing the number of livestock. Reasonable grazing is related to the development and stability of regional economy, and requires comprehensive consideration from multiple perspectives such as society, economy, and technology (Chen et al., 2024; Guo and Chen, 2024). Therefore, reasonable grassland management policies (e.g., rotational grazing, grazing rest, and control of grazing intensity) should be formulated.

Spatially, the overloaded and severely overloaded areas were mainly distributed in northern areas in the agro-pastoral transition zone of northern China, which is consistent with the findings of Guo et al. (2021). These areas are characterized by typical arid and semi-arid climates with low and highly variable precipitation. Limited by scarce water resources and low above-ground biomass, these areas are highly vulnerable to overgrazing (Zhang et al., 2022). With the global climate change, frequent occurrence of weather extremes further accelerates the rate of grassland degradation, increases the pressure on grassland ecosystems, and ultimately exacerbates livestock

overload in these areas (Cheng et al., 2014; Zhu et al., 2023; Xu, 2024). As the population continues to grow and urbanization accelerates, human demand for livestock products continues to increase (Liu et al., 2006; Erdaw, 2023). This phenomenon prompts herders to further expand their farming scale, rendering the regional forage-livestock balance overloaded.

4.3 Prediction of potential GCC

Potential GCC would show a downward trend from 2024 to 2030, but would increase in 2028 under SSP5-8.5 scenario. The main reason may be that the elevated CO_2 concentration in this scenario promotes grass photosynthesis (Chai and Hu, 2024), which increases NPP and consequently potential GCC. In high latitudes of the agricultural and pastoral zones in northern China, warm temperatures lengthen the growing season (Zhang et al., 2022), which also indirectly increases the potential GCC under this scenario. However, under SSP2-4.5 scenario, potential GCC would decrease in 2028. The main reason may be that the moderate warming under this scenario leads to increased evapotranspiration and the increase in precipitation is not sufficient to compensate for the water loss (Xiang et al., 2021; Guo et al., 2023), resulting in water stress. Hence, potential GCC in this scenario decreases. In addition, the increased frequency of drought events under this scenario (Li et al., 2020) is not conducive to a high NPP, leading to a decrease in potential GCC in this area. Given that potential GCC in the future mainly shows a downward trend, reasonable livestock numbers should be controlled and effective management policies should be implemented to avoid further damage and further degradation of grassland ecosystems caused by overgrazing. The prediction results indicated that future high-value areas of potential GCC are mainly distributed in southern area of the agricultural and pastoral transition zone in northern China. Adequate precipitation and favorable temperatures in this area help to increase potential GCC. Under the principle of coordinating economic development and environmental protection, grassland management policies should be optimized by spatial configuration of GCC, which is necessary for the harmonization of economic and ecological development.

4.4 Limitations and future prospects

The analysis of spatiotemporal variation of GCC in the agro-pastoral transition zone of northern China and its influencing factors provides a macro perspective on long-term GCC dynamics. However, the use of various data sources, such as meteorological data and economic data, and the lack of field measurements for verification may lead to certain deviations in the results. Strengthening the verification test in subsequent studies is necessary. In addition, this study utilized the CMIP6 dataset to predict potential GCC in the future. Effects of precipitation and temperature on GCC were considered. However, in some areas, the time series of temperature and precipitation distribution (whether rain and heat coincide or not), wind speed, and solar radiation were becoming increasingly significant factors affecting GCC. Owing to current difficulty in obtaining these data, improvements in collection and expansion of data sources are urgently needed to provide a solid foundation for in-depth and comprehensive research.

5 Conclusions

Multi-source remote sensing data were used to analyze GCC and forage-livestock balance in the agro-pastoral transition zone of northern China. Results showed an overall upward trend in GCC from 2000 to 2022, with high-values areas predominantly located in eastern and southern areas. These trends were primarily influenced by precipitation and temperature, supporting the idea that precipitation was the most important factor influencing GCC in arid and semi-arid grasslands. Areas with high GCC in southern areas of the agro-pastoral transition zone of northern China might be related to high annual cumulative temperature of these areas, further emphasizing the effect of temperature on GCC. The forage-livestock balance was overloaded in most parts of the study area. Future GCC estimation calculated by selected model generally showed a downward

trend, and areas with high GCC were mainly distributed in the south. These prediction results provide a theoretical basis for the optimization of grassland management policy in the future.

Conflict of interest

The authors declare that they have no known competing financial interests or personal relationships that could have appeared to influence the work reported in this paper.

Acknowledgements

This study was supported by the National Natural Science Foundation of China (42271309) and the Natural Science Foundation of Shaanxi Province (2024JC-YBMS-194). The authors are very grateful to the anonymous reviewers and editors for their critical review and comments.

Author contributions

Conceptualization: LIU Huan, AI Zemin; Data curation: LIU Huan, YAO Yuyan, CAO Tian; Methodology: LIU Huan, YAO Yuyan, ZHANG Yuanyuan; Investigation: LI Qingqing; Software: LIU Huan, HOU Mengjia; Formal analysis: CAO Yong, LI Qingqing; Writing - original draft preparation: LIU Huan; Writing - review and editing: LIU Huan, AI Zemin; Funding acquisition: AI Zemin, DANG Xiaohu; Resources: YAO Yuyan, HU Haoli; Supervision: AI Zemin. All authors approved the manuscript.

References

Ba W R, Qiu H T, Cao Y G, et al. 2023. Spatiotemporal characteristics prediction and driving factors analysis of NPP in Shanxi Province covering the period 2001–2020. Sustainability, 15(15): 12070, doi: 10.3390/su151512070.

Bai S T, Yang J C, Zhang Y B, et al. 2022. Evaluating ecosystem services and trade-offs based on land-use simulation: A case study in the farming–pastoral ecotone of northern China. Land, 11(7): 1115, doi: 10.3390/land11071115.

Brunsdon C, Fotheringham A S, Charlton M E. 1996. Geographically weighted regression: A method for exploring spatial nonstationarity. Geographical Analysis, 28(4): 281–298.

Chai Y F, Hu Y. 2024. Characteristics and drivers of vegetation productivity sensitivity to increasing CO_2 at northern middle and high latitudes. Ecology Evolution, 14(5): e11467, doi: 10.1002/ece3.11467.

Chen N, Jayaprakash C, Yu K L, et al. 2018. Rising variability, not slowing down, as a leading indicator of a stochastically driven abrupt transition in a dryland ecosystem. The American Naturalist, 191(1): E1–E14, doi: 10.1086/694821.

Chen Q G. 2005. Key pasture, seasonal grazing and sustainable development of grassland animal husbandry production in China. Acta Prataculturae Sinica, 14(4): 29–34. (in Chinese)

Chen Q G. 2008. Current status and development of grassland monitoring in China. Pratacultural Science, 25(2): 29–38. (in Chinese)

Chen S R, Wang S X, Zhou Y. 2008. Estimation of Chinese grassland productivity using remote sensing. Transactions of the CSAE, 24(1): 208–212. (in Chinese)

Chen T, Zheng H, Chen J, et al. 2024. Novel intelligent grazing strategy based on remote sensing, herd perception and UAVs monitoring. Computers and Electronics in Agriculture, 219: 108807, doi: 10.1016/j.compag.2024.108807.

Chen Z F, Wang W G, Fu J Y. 2020. Vegetation response to precipitation anomalies under different climatic and biogeographical conditions in China. Scientific Reports, 10: 830, doi: 10.1038/s41598-020-57910-1.

Cheng C G, Zhou W, Chen Y Z, et al. 2014. Quantitative assessment of the contributions of climate change and human activities on global grassland degradation. Environmental Earth Sciences, 72: 4273–4282.

Dai E F, Wang Y H. 2020. Spatial heterogeneity and driving mechanisms of water yield service in the Hengduan Mountain region. Acta Geographica Sinica, 75(3): 607–619. (in Chinese)

Dai L W, Tang H P, Pan Y L, et al. 2024. Assessment of ecosystem stability in the agro-pastoral transitional zone for local sustainable management: A case study in Duolun County, northern China. Ecological Indicators, 162: 112018, doi: 10.1016/j.ecolind.2024.112018.

De Leeuw J, Rizayeva A, Namazov E, et al. 2019. Application of the MODIS MOD 17 net primary production product in grassland carrying capacity assessment. International Journal of Applied Earth Observation and Geoinformation, 78: 66–76.

Dong S K, Jiang Y, Huang X X. 2002. Suitability degree of grassland grazing and strategies for pasture management. Resources

Science, 24(6): 35–41. (in Chinese)

Du Q Q, Sun Y F, Guan Q Y, et al. 2022. Vulnerability of grassland ecosystems to climate change in the Qilian Mountains, Northwest China. Journal of Hydrology, 612: 128305, doi: 10.1016/j.jhydrol.2022.128305.

Du Q Q, Sun Y F, Guan Q Y, et al. 2024. Theoretical carrying capacity of grasslands and early warning for maintaining forage-livestock balance in the Qilian Mountains, Northwest China. Plant and Soil, 498: 225–241.

Dusenge M E, Duarte A G, Way D A. 2019. Plant carbon metabolism and climate change: Elevated CO_2 and temperature impacts on photosynthesis, photorespiration and respiration. New Phytologist, 221(1): 32–49.

Erb K-H, Kastner T, Plutzar C, et al. 2018. Unexpectedly large impact of forest management and grazing on global vegetation biomass. Nature, 553: 73–76.

Erdaw M M. 2023. Contribution, prospects and trends of livestock production in sub-Saharan Africa: A review. International Journal of Agricultural Sustainability, 21(1): 2247776, doi: 10.1080/14735903.2023.2247776.

Fenetahun Y, Yuan Y, Xu X W, et al. 2022. Borana rangeland of southern Ethiopia: Estimating biomass production and carrying capacity using field and remote sensing data. Plant Diversity, 44(6): 598–606.

Fuchslueger L, Bahn M, Hasibeder R, et al. 2016. Drought history affects grassland plant and microbial carbon turnover during and after a subsequent drought event. Journal of Ecology, 104(5): 1453–1465.

Guevara J, Cavagnaro J, Estevez O, et al. 1997. Productivity, management and development problems in the arid rangelands of the central Mendoza plains (Argentina). Journal of Arid Environments, 35(4): 575–600.

Guo Y, Jia Z B, Zhang Q, et al. 2021. Study on the spatiotemporal dynamics of forage-livestock balance in Hulunbuir Grassland of Inner Mongolia based on remote sensing data. Chinese Journal of Grassland, 43(4): 30–37. (in Chinese)

Guo Y J, Chen Y Y. 2024. A review of the impact of grazing on grassland ecosystems: Research progress and prospects. Advances in Resources Research, 4(3): 455–473.

Guo Z C, Li Y Q, Wang X Y, et al. 2023. Remote sensing of soil organic carbon at regional scale based on deep learning: A case study of agro-pastoral ecotone in northern China. Remote Sensing, 15(5): 3846, doi: 10.3390/rs15153846.

Hahn C, Lüscher A, Ernst-Hasler S, et al. 2021. Timing of drought in the growing season and strong legacy effects determine the annual productivity of temperate grasses in a changing climate. Biogeosciences, 18(2): 585–604.

He S Y, Xiong K N, Song S Z, et al. 2023. Research progress of grassland ecosystem structure and stability and inspiration for improving its service capacity in the Karst desertification control. Plants, 12(4): 770, doi: 10.3390/plants12040770.

Huang L, Ning J, Zhu P, et al. 2021. The conservation patterns of grassland ecosystem in response to the forage-livestock balance in North China. Journal of Geographical Sciences, 31: 518–534.

Huang L, Wang D J, Yao L H, et al. 2019. Primary limitation on vegetation productivity shifts from precipitation in dry years to nitrogen in wet years in a degraded arid steppe of Inner Mongolia, northern China. Journal of Soils and Sediments, 19: 544–556.

Jiang H L, Xu X, Guan M X, et al. 2020. Determining the contributions of climate change and human activities to vegetation dynamics in agro-pastoral transitional zone of northern China from 2000 to 2015. Science of the Total Environment, 718: 134871, doi: 10.1016/j.scitotenv.2019.134871.

Jin X M, Han G D. 2010. Evaluation of rangeland condition and estimation of grazing capacity in *Stipa baicalensis* steppe. Journal of Northeast Normal University, 42(1): 117–122. (in Chinese)

Jin Y X, Xu B, Yang X C, et al. 2011. Remote sensing dynamic estimation of grass production in Xilinguole, Inner Mongolia. Scientia Sinica, 41(12): 1185–1195. (in Chinese)

Jordon M W, Buffet J C, Dungait J A, et al. 2024. A restatement of the natural science evidence base concerning grassland management, grazing livestock and soil carbon storage. Proceedings of the Royal Society B, 291(2015): 20232669, doi: 10.1098/rspb.2023.2669.

Li C J, Fu B J, Wang S, et al. 2023. Climate-driven ecological thresholds in China's drylands modulated by grazing. Nature Sustainability, 6: 1363–1372.

Li M H, Wang J L, Li K, et al. 2024. Assessment of grazing livestock balance on the Eastern Mongolian Plateau based on remote sensing monitoring and grassland carrying capacity evaluation. Scientific Reports, 14: 32151, doi: 10.1038/s41598-024-84215-4.

Li S Y, Miao L J, Jiang Z H, et al. 2020. Projected drought conditions in northwest China with CMIP6 models under combined SSPs and RCPs for 2015–2099. Advances in Climate Change Research, 11(3): 210–217.

Li T, Cui L Z, Scotton M, et al. 2022. Characteristics and trends of grassland degradation research. Journal of Soils and Sediments, 22: 1901–1912.

Li W J, Jiu C L, Tan Z H, et al. 2012. Natural grassland productivity and the livestock-feeds balance in Qinghai Province.

Resources Science, 34(2): 367–372. (in Chinese)

Liu J H, Huang X, He X Y, et al. 2018. Estimation of grassland yield and carrying capacity in Qinghai Province based on MODIS data. Pratacultural Science, 35(10): 2520–2529. (in Chinese)

Liu L S, Zhang Y L, Bai W Q, et al. 2006. Characteristics of grassland degradation and driving forces in the source region of the Yellow River from 1985 to 2000. Journal of Geographical Sciences, 16: 131–142.

Liu Y H, Shi L, Chang H, et al. 2021. Analysis of driving factors that influence the pattern and quality of the ecosystem in Xilingol League. Acta Prataculturae Sinica, 30(12): 17–26. (in Chinese)

Ma B X, Jing J L, Liu B, et al. 2023. Assessing the contribution of human activities and climate change to the dynamics of NPP in ecologically fragile regions. Global Ecology and Conservation, 42: e02393, doi: 10.1016/j.gecco.2023.e02393.

Mai X H, Zhang Y J, Zhang Y J, et al. 2013. Research progress of grassland feed-animal balance at home and abroad. Asian Agricultural Research, 5(12): 73–76.

Petermann J S, Buzhdygan O Y. 2021. Grassland biodiversity. Current Biology, 31(19): R1195–R1201, doi: 10.1016/j.cub.2021.06.060.

Qi X L, Xu H J, Teng R Y, et al. 2024. Ecological restoration largely alleviates livestock grazing pressure in a montane grassland. Journal of Cleaner Production, 467: 143044, doi: 10.1016/j.jclepro.2024.143044.

Qian S, Wang L Y, Gong X F. 2012. Climate change and its effects on grassland productivity and carrying capacity of livestock in the main grasslands of China. The Rangeland Journal, 34(4): 341–347.

Qu Y B, Zhao Y Y, Ding G D, et al. 2021. Spatiotemporal patterns of the forage-livestock balance in the Xilin Gol Steppe, China: Implications for sustainably utilizing grassland-ecosystem services. Journal of Arid Land, 13(2): 135–151.

Romero-Ruiz A, Monaghan R, Milne A, et al. 2023. Modelling changes in soil structure caused by livestock treading. Geoderma, 431: 116331, doi: 10.1016/j.geoderma.2023.116331.

Sedgwick P. 2012. Pearson's correlation coefficient. British Medical Journal, 345: e4483, doi: 10.1136/bmj.e4483.

Shi Y, Brierley G, Perry G L, et al. 2024. An improved approach to estimate stocking rate and carrying capacity based on remotely sensed phenology timing. Remote Sensing, 16(11): 1991, doi: 10.3390/rs16111991.

Song X Y, Xing Q M, Chang S J, et al. 2018. Comprehensive evaluation on bearing capacity of desert steppe in Inner Mongolia. Journal of Anhui Agricultural Sciences, 46(14): 93–96. (in Chinese)

Su D X, Meng Y D, Wu B G. 2002. Calculation of Reasonable Livestock Carrying Capacity of Natural Grassland in NY/T635-2002. Beijing: China Agriculture Press. (in Chinese)

Su R N, Zu J X, Jin H, et al. 2017. Changes in grassland productivity and livestock carrying capacity in Inner Mongolia. Ecology Environmental Sciences, 26(4): 605–612. (in Chinese)

Umuhoza J, Jiapaer G, Yin H M, et al. 2021. The analysis of grassland carrying capacity and its impact factors in typical mountain areas in Central AsiaA case of Kyrgyzstan and Tajikistan. Ecological Indicators, 131: 108129, doi: 10.1016/j.ecolind.2021.108129.

Wang G Q, Liu X Y. 2017. Discussion on the balance of grassland and livestock in Inner Mongolia. Ecological Economy, 33(4): 160–164. (in Chinese)

Wang J F, Xu C D. 2017. Geodetector: Principle and prospective. Acta Geographica Sinica, 72(1): 116–134. (in Chinese)

Wang Q X, Okadera T, Nakayama T, et al. 2024a. Estimation of the carrying capacity and relative stocking density of Mongolian grasslands under various adaptation scenarios. Science of the Total Environment, 913: 169772, doi: 10.1016/j.scitotenv.2023.169772.

Wang Z Y, Zhou Y F, Sun X Y, et al. 2024b. Estimation of NPP in Huangshan district based on deep learning and CASA model. Forests, 15(8): 1467, doi: 10.3390/f15081467.

Wei W R, Zhang Y, Tang Z M, et al. 2022. Suitable grazing during the regrowth period promotes plant diversity in winter pastures in the Qinghai-Tibetan Plateau. Frontiers in Ecology Evolution, 10: 991967, doi: 10.3389/fevo.2022.991967.

Wen Y Y, Liu X P, Xin Q C, et al. 2019. Cumulative effects of climatic factors on terrestrial vegetation growth. Journal of Geophysical Research: Biogeosciences, 124(4): 789–806.

Xiang Y Y, Wang Y, Chen Y N, et al. 2021. Impact of climate change on the hydrological regime of the Yarkant River Basin, China: An assessment using three SSP scenarios of CMIP6 GCMs. Remote Sensing, 14(1): 115, doi: 10.3390/rs14010115.

Xiong F Q, Zhang J L, Guo J, et al. 2025. Temporal and spatial changes in grass-animal balance in Wensu County, 2000–2022. Pratacultural Science, 42(1): 247–259. (in Chinese)

Xu B, Yang X C. 2009. Calculation of grass production and balance of livestock carrying capacity in rangeland region of Northeast China. Geographical Research, 28(2): 402–408. (in Chinese)

Xu B, Yang X C, Jin Y X, et al. 2012. Monitoring and evaluation of grassland-livestock balance in pastoral and semi-pastoral

counties of China. Geographical Research, 31(11): 1998–2006. (in Chinese)

Xu H J, Zhao C Y, Wang X P. 2020. Elevational differences in the net primary productivity response to climate constraints in a dryland mountain ecosystem of northwestern China. Land Degradation & Development, 31(15): 2087–2103.

Xu X F. 2024. Frequent occurrence of extreme weather and out-of-balance climate systems. The Innovation Geoscience, 2(1): 100049, doi: 10.59717/j.xinn-geo.2024.100049.

Yan L Y, Kong L Q, Wang L J, et al. 2024. Grass-livestock balance under the joint influences of climate change, human activities and ecological protection on Tibetan Plateau. Ecological Indicators, 162: 112040, doi: 10.1016/j.ecolind.2024.112040.

Yan N N, Zhu W W, Wu B F, et al. 2023. Assessment of the grassland carrying capacity for winter-spring period in Mongolia. Ecological Indicators, 146: 109868, doi: 10.1016/j.ecolind.2023.109868.

Yang H L, Yao B, Su Y Z, et al. 2024. Distribution pattern of soil physical and chemical properties of plantation forest in northern agropastoral ecotone. Journal of Desert Research, 44(2): 283–294. (in Chinese)

Yang Y J, Wang K, Liu D, et al. 2020. Effects of land-use conversions on the ecosystem services in the agro-pastoral ecotone of northern China. Journal of Cleaner Production, 249: 119360, doi: 10.1016/j.jclepro.2019.119360.

Yang Z L, Yang G H. 2000. Potential productivity and livestock carrying capacity of high-frigid grassland in China. Resources Science, 22(4): 72–77. (in Chinese)

Yu C L, Liu D, Zhao H Y. 2021. Evaluation of the carbon sequestration of Zhalong Wetland under climate change. Journal of Geographical Sciences, 31: 938–964.

Zeng Z G, Bi J H, Li S R, et al. 2014. Effects of habitat alteration on lizard community and food web structure in a desert steppe ecosystem. Biological Conservation, 179: 86–92.

Zhang G G, Kang Y M, Han G D, et al. 2011. Effect of climate change over the past half century on the distribution, extent and NPP of ecosystems of Inner Mongolia. Global Change Biology, 17(1): 377–389.

Zhang W H, Jia Z B, Zhuo Y, et al. 2016. Space dynamic change of pasture amount and influence factors analysis in Xilin Gol Grassland. Journal of Earth Environment, 7(2): 163–172. (in Chinese)

Zhang X Z, Li M, Wu J S, et al. 2022. Alpine grassland aboveground biomass and theoretical livestock carrying capacity on the Tibetan Plateau. Journal of Resources Ecology, 13(1): 129–141.

Zhang Z, Hu B Q, Jiang W G, et al. 2023. Spatial and temporal variation and prediction of ecological carrying capacity based on machine learning and PLUS model. Ecological Indicators, 154: 110611, doi: 10.1016/j.ecolind.2023.110611.

Zhou G S, Zheng Y R, Chen S Q. 1998. NPP model of natural vegetation and its application in China. Scientia Silvae Sinicae, 34(5): 2–11. (in Chinese)

Zhu P, Huang L, Zhai J, et al. 2022. Changing trends in grazing pressure in key ecological function area of the agro-pastoral zone. Pratacultural Science, 39(6): 1269–1279. (in Chinese)

Zhu Q, Chen H, Peng C H, et al. 2023. An early warning signal for grassland degradation on the Qinghai-Tibetan Plateau. Nature Communications, 14: 6406, doi: 10.1038/s41467-023-42099-4.